IUST Iran University of Science and Technology

Iranian Journal of Electrical and Electronic Engineering

Journal Homepage: ijeee.iust.ac.ir

Research Paper

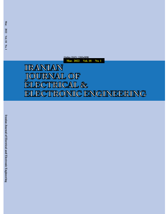

Lightning Evaluation of Overhead Transmission Line Protected by EGLA

M. Khodsuz*(C.A.)

Abstract: Lightning is the main factor of outage and insulation breakdown of power system. The lightning event can produce dangerous overvoltage, equipment failures, and power supply interruption. In this paper, externally gapped Line arresters (EGLAs) performances have been investigated to evaluate the lightning performances of a typical 63 kV transmission line. A probabilistic analysis has been done to study the EGLA performance in transmission line by Monte-Carlo method. The results show the EGLA performance dependency to soil resistivity and lightning strike parameters.

Keywords: Externally Gapped Line Arrester, Insulation Breakdown, Nonlinear Resistor, Overvoltage.

1 Introduction

LIGHTNING is the main factor of outage and insulation failure power system. The lightning event can produce dangerous overvoltage, equipment failures, power supply interruption. Surge arresters (SAs) have been used widely in utilities for switching or lightning surges energy stress elimination. Also, it can be able to limit surge magnitude to a satisfactory margin. The major factors of unpredicted outages and equipment failures are switching and lightning over-voltages [1-4].

Lightning surges may strike to the shield wires, towers, and even the ground and cause induction voltage. Direct lightning strikes are a common reason for transmission line outages. Three mechanisms are responsible for these outages, specifically the flashover through insulator strings, the back-flashover (BF), and the mid-span flashover. The first mechanism takes place due to the lightning strikes to the phase conductor and this is due to the absence of shielding wires or due to a shielding failure (SF). It can cause an insulation flashover for transmission lines [5-7]. Surge arresters installation in the transmission line will be an appropriate solution to reduce insulation failures, lightning failure outage rate (LFOR) and also improves network reliability [8, 9].

Surge arresters technology is divided into two groups including externally gapped line arrester (EGLA) and surge arrester without the external air gap. The EGLA consists of two parts including zinc oxide varistors and external air gap. In EGLA, ZnO disks are not normally energized and thus will not be destroyed under normal operating conditions. Nowadays, owing to specific advantages of externally gapped line arresters such as no corrosion, successful reclosing process, and superior protecting characteristic thanks to the residual voltage with lower amplitude, this type of surge arrester is widely implemented. However, EGLA has lower performance during overvoltage caused by switching [10-13].

So far, some researches have been performed to evaluate the transmission line performances against surges and also the arresters failure risk calculation. By SA installation, the probabilities of insulation failure and outage rates are reduced. But owing to the energy absorption capability of the SA, the probability of arrester failure happens that may cause network interruption or equipment damaging. The presented methods are based on either Monte-Carlo simulation to calculate the failure probability [14-16].

A 63 kV line double circuit flashover performance has been studied using EMTP software [15]. The influence of tower footing resistance, lightning current amplitudes

Iranian Journal of Electrical and Electronic Engineering, 2022.
Paper first received 14 December 2021, revised 06 March 2022, and accepted 13 May 2022.
* The author is with the Faculty of Electrical and Computer Engineering, University of Science and Technology of Mazandaran, Behshahr, Iran.
E-mail: m.khodsouz@mazust.ac.ir.
Corresponding Author: M. Khodsuz.
https://doi.org/10.22068/IJEEE.18.2.2370

and power frequency voltage have been considered. The back-flashover in 220 kV transmission line is studied in [16] for various current waveforms and tower footing resistances. For a suitable protective system design, the energy absorption capacity of the arrester must be calculated exactly [17-19].

Surge arresters' performances against lightning have been investigated in many researches but the EGLA performances have not been investigated comprehensively. Equipped transmission lines with EGLAs can vary the transient wave traveling impedance [12, 13]. The influences of lightning parameters on the EGLA discharge energy and its expected life have not been considered in the literature. In this paper, a probabilistic investigation has been done on the EGLA performance and its lifetime. Furthermore, lightning flashes effect on the energy stress experienced by EGLAs has been taken into account. To this aim, the Monte-Carlo method has been applied for performing the required probabilistic studies. For assessment, a typical 63 kV transmission line has been modeled in EMTP -ATP software linked with MATLAB software.

The paper is prepared as follows: the modeling of transmission line components, surge arrester and grounding resistor in EMTP-ATP software are discussed in Sections 2 and 3. Simulation results are represented in Section 4. The conclusion is explained in Section 5.

2 Lightning Parameters

2.1 Lightning Current Parameters

The lightning parameters including current amplitude (I_p), rise time (t_f), and tail time (t_h) are estimated using a log-normal distribution as follows [20]:

$$f(y) = \frac{1}{\sigma_{\ln y}\sqrt{2\pi}y}\exp\left[-\frac{(\ln y - \ln \bar{y})^2}{2\sigma_{\ln y}{}^2}\right] \tag{1}$$

where $\sigma_{\ln x}$ and $\bar{y}$ are the standard deviation and average of y variable, respectively.

The statistical value of lightning parameters has been represented in Table 1 [20] to simulate the distribution function of lightning parameters.

Several expressions have been suggested to represent the lightning waveform [21]. Heidler model is one of the most common models and given by:

$$i(t) = \frac{i_p}{\eta}\frac{K^n}{1+K^n}e^{-t/\tau_2} \tag{2}$$

where i_p is current amplitude, n is current steepness factor and η is correction factor and $K = t/\tau_1$ respectively. τ_1 and τ_2 are time constants corresponding to the rise time and tail time of lightning waveform, respectively [21, 22].

3 Transmission Line Equipment Model

3.1 Line and Tower Modeling

The 63 kV transmission line has been modeled by four spans with a length of 400 meters on each side of the struck point. Each span has been simulated by J. Marti's model in EMTP-ATP software which is a frequency-dependent line model. To prevent the reflection, that can affect the simulated overvoltage, a line with a length of 30 km is inserted on each side of the simulated transmission line. Transmission towers were modeled based on an actual tower for a 63 kV transmission line, as illustrated in Fig. 1(a). The multistory model has been used to simulate the studied tower [23]. As shown in Fig. 1(b), Z_t has been utilized to model the impedance of different parts of the tower and the R-L parallel branch models traveling-wave attenuation and distortion [23].

3.2 Insulator String and Breakdown Modeling

The insulator string model and flashover are necessary for insulation breakdown investigation. For this purpose, the leader progression model has been represented. In this model, the insulator string has been revealed by a capacitor parallel with a voltage-controlled switch. When the insulator string voltage exceeds the corona initiation voltage, streamers originate along the insulator. If the voltage remains high, a leader channel will be created and a failure happens. The leader propagation time is the essential component of the total breakdown time and can be calculated as follows [24]:

Table 1 Statistical data of lightning parameters.

parameters	First stroke		Subsequent stroke	
	Standard deviation	Average	Standard deviation	Average
I_p [kA]	0.46	31	0.641	13
t_f [μs]	0.54	5	0.66	0.31
t_h [μs]	0.56	70	0.67	20

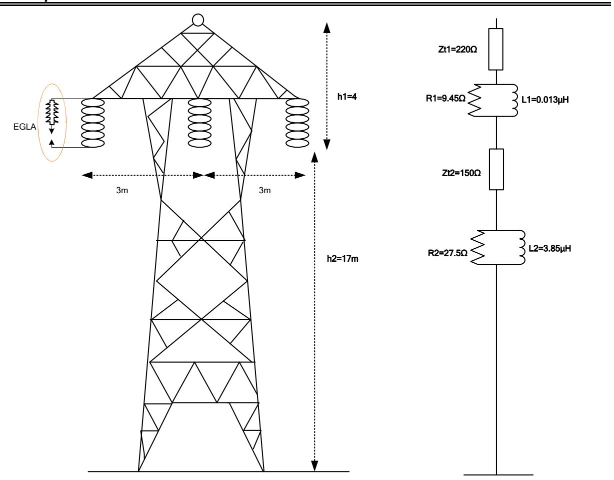

(a) (b)

Fig. 1 A schematic diagram of a 63 kV transmission tower and its multistory model.

$$\frac{dl}{dt} = K_l v_{(t)} \left[\frac{v_{(t)}}{h-l} - e_{l0} \right] \tag{3}$$

where $v_{(t)}$ is the voltage across insulator in kV, l is the leader length and these two parameters are calculated during simulation. h is the insulator string length and it is considered 1 m in 63 kV transmission line. K_l is 1.3 ($m^2.kV^{-2}.s^{-1}$) and e_{l0} is 580 kV/m. in addition, the insulator numbers were 5.

3.3 Grounding Resistance Modeling

The behavior of the grounding system affects the flashover probability of the insulator strings. Since lightning strike is discharged through grounding, ground impedance modeling is important. The grounding system is modeled as a static model (A constant resistance) and nonlinear resistance model with a soil ionization effect. In the nonlinear resistance model, the tower footing impedance (as shown in (4)) has been exhibited by a nonlinear resistance whereby the soil ionization changes according to the passing current through the tower footing [25].

$$R_t = \frac{R_0}{\sqrt{1+\frac{I}{I_g}}}, \quad I_g = \frac{E_0 \rho}{2\pi R_0^{\,2}} \tag{4}$$

where R_t is the tower footing resistance, R_0 is footing resistance at low current and low frequency, ρ (Ω.m) is the soil resistivity, I is the lightning strike current across the resistance, I_g is the limiting current to originate enough soil ionization, and E_0 is the voltage gradient. The R_0 values for different soil resistivities have been shown in Table 2.

3.4 EGLA Modeling

An external air gap arrester consists of two parts including zinc oxide varistors and external air gap. It is important to regulate the gap of this type of arrester. This gap must be large enough to be able to withstand the transient overvoltages and also small enough to spark over before the insulator flashes over. The smallest suitable gap of an EGLA has been regulated by the voltage, probable temporary overvoltage, and a safety factor (SF_1). The maximum satisfactory gap has been defined by the critical flashover voltage. If the gap spacing is lower than the smallest acceptable level, the flashover risk increases which causes during the temporary overvoltage. If the gap has been designed higher than the maximum amount, it causes insulator breakdown before the gap sparks [10-13]. For modeling the active part, which includes zinc oxide varistors, the IEEE frequency-dependent model has been used. The represented model of the IEEE Working Group 3.4.11 has been shown in Fig. 2 which includes five parameters (R_0, L_0, L_3, R_3, and C). The terminal-to-terminal capacitance of the arrester has been modeled as C in the represented model. The filter impedance (L_3 parallel with R_3) becomes low during applied slow front surge waves and so the non-linear resistances A_0 and A_1 are in parallel. The filter impedance in the represented model is high for fast front waves and consequently, the lightning current passes through the non-linear resistance A_0. The nonlinear V-I characteristics of A_0 and A_1 have been computed by given values in Table 3.

The minimum adequate gap of an EGLA is calculated by three features: system voltage, expected temporary overvoltage (TOV), and SF_1. The minimum voltage that causes EGLA gap flashover is:

$$V = \frac{V_{sys}}{1.73} \times TOV \times SF_1 \quad [kV_{rms}] \tag{5}$$

where V is minimum power frequency flashover voltage, V_{sys} is system voltage and TOV and SF_1 are 1.4 and 1.2, respectively.

For modeling the active part, which includes zinc oxide varistors, the IEEE frequency-dependent model has been used. Moreover, Eq. (6) has been applied to adjust the EGLA gap, which is in series with the IEEE model [13].

Table 2 R_0 values for different soil resistivities.

Soil resistivity [Ω.m]	R_0 [Ω]
100	10
250	25
500	50
750	75
1000	100

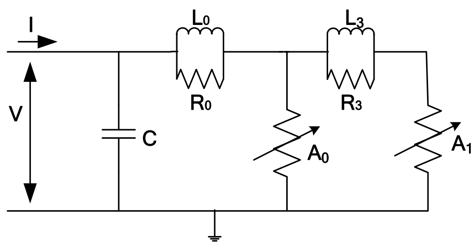

Fig. 2 Metal-oxide surge arrester IEEE model.

Table 3 V-I characteristics for A_0 and A_1 (V_{10} is discharge voltage in kV for 10 kA 8/20 µs impulse current).

Current [kA]	Voltage (per unit of V_{10})	
	A_0	A_1
0.01	0.875	-
0.1	0.963	0.769
1	1.050	0.850
2	1.088	0.894
4	1.125	0.925
6	1.138	0.938
8	1.169	0.956
10	1.188	0.969
12	1.206	0.975
14	1.231	0.988
16	1.250	0.994
18	1.281	1
20	1.313	1.006

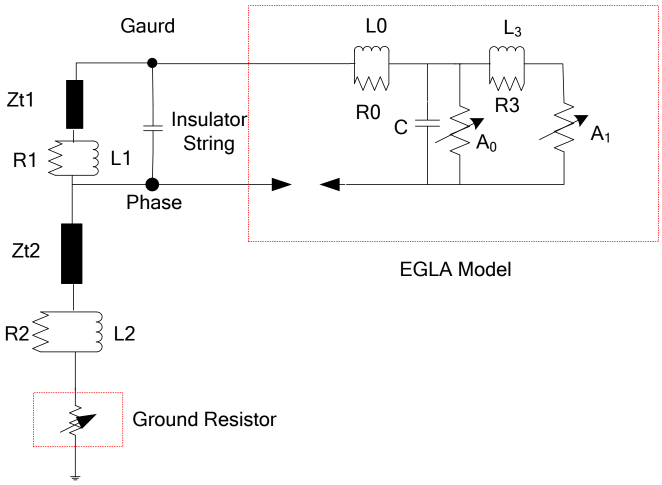

Fig. 3 The EGLA model in the EMTP-ATP software.

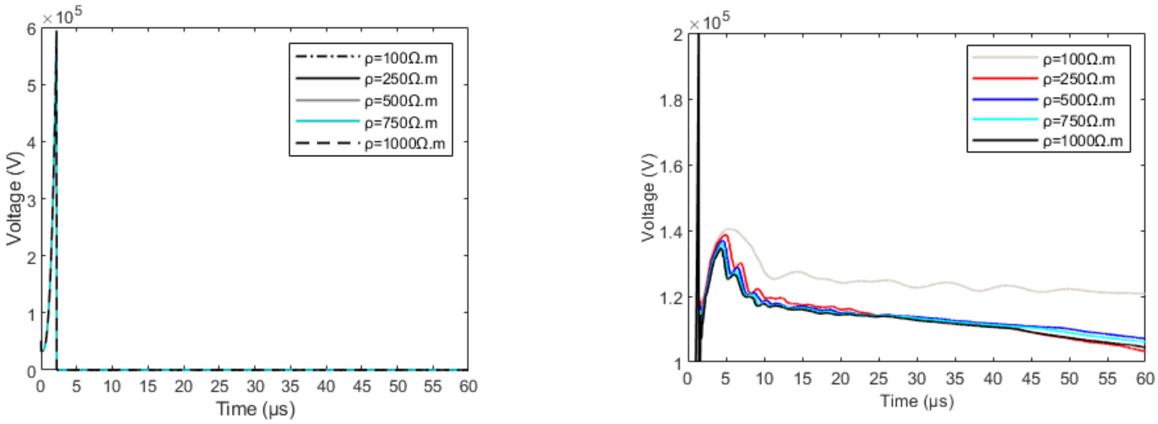

Fig. 4 Overvoltage across insulator string caused by the lightning stroke to phase conductor (31 kA 5/70 μs); a) without EGLA and b) with EGLA.

$$d_{\max} = \frac{V_{CFO} \times 0.85}{e_0},$$
$$d_{\min} = 39.37\left[\frac{e^{\frac{V}{750}} - 1}{0.55}\right]^{0.833} \quad \text{[Inches]} \tag{6}$$

where $d_{\min}$ and $d_{\max}$ are minimum and maximum EGLA gap, respectively, V_{CFO} is critical voltage of insulator string and e_0 is corona initiation gradient [10, 13]. Fig. 3 shows the EGLA model in EMTP-ATP software.

4 Simulation Results

The 63 kV transmission line has been simulated to study EGLA performances. The towers have been simulated by the multistory model, as explained in Section 3.1. The insulator strings have been modeled based on the leader propagation model of Section 3.2. The IEEE model has been used to model EGLA active part and its series external gap has been modeled based on (5), as explained in Section 3.4.

The following section presents the EGLA performance for the 63 kV transmission line. The lightning surges have been struck on top of the middle tower (wire shield) and at the mid-span. The influence of tower footing resistance on the line lightning performance has been also investigated to more analyze EGLA performance for eliminating transmission line outages initiated from flashover.

4.1 Overvoltage Investigation for the Lightning Strokes to Phase Conductor

Fig. 4 represents insulator string overvoltage caused by the lightning strokes 31 kA, 5/70 μs, to A phase conductor. In this figure, nonlinear resistance has been considered. According to the results, the insulator string overvoltage value is affected by EGLA installation. As shown in Fig. 4(a), insulation breakdown has happened due to the high lightning amplitude without EGLA installation on the stroked tower .Also, electrical failure has occurred in all cases and so all figures have been overlapped. In Fig. 4(b), the insulator flashover has been limited by EGLA installing in parallel with the struck tower's insulator string and there was no

Table 4 The insulator string overvoltages across for static and nonlinear resistors (with EGLA installation).

Soil resistivity [Ω.m]	Overvoltage values [kV]	
	Static resistor	Nonlinear resistor
100	140	140.4
250	138.1	138.8
500	135.7	137
750	131.5	135.9
1000	131	134.7

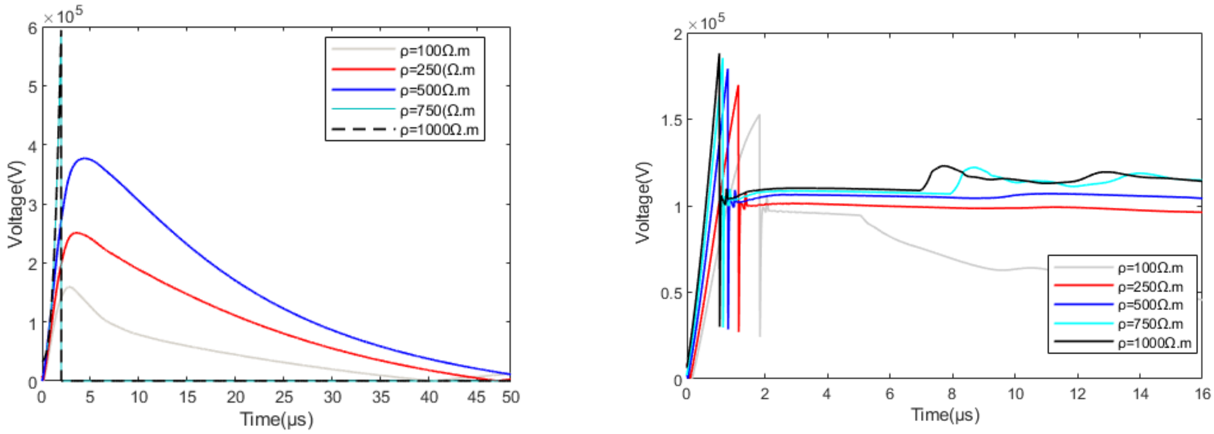

(a) (b)

Fig. 5 Overvoltage across insulator string caused by the lightning stroke to shielding wire (31 kA 5/70 μs); a) without EGLA and b) with EGLA.

insulation breakdown. Increasing soil resistivity from 100 Ω.m to 1000 Ω.m results in less overvoltage magnitude and the results indicate that the overvoltage amplitude is influenced by the soil resistivity. By decreasing soil resistivity, more discharge current can flow through surge arrester (due to less grounding resistance), and result in more insulator overvoltage amplitude.

The overvoltages values across the insulator string associated with static and nonlinear resistances have been depicted in Table 4. As shown in reported results, the overvoltages amplitudes for nonlinear resistors are higher than the static ones. For the nonlinear resistor, the soil electrical parameters depend on the soil ionization which will result in more passing current from the tower footing. This assistances to increase the lightning overvoltage across the insulator string. Also, by soil resistivity reduction, more discharge current flows through the EGLA and results in higher overvoltage magnitudes.

4.2 Overvoltage Investigation for the Lightning Strokes to Shielding Wire

The tower footing resistance was changed between 100 Ω.m to 1000 Ω.m to show its dependency on the EGLA performances against the lightning strokes to shielding wire. In this section, tower footing resistance has been modeled by a nonlinear resistance depending on the flowing current magnitude. Fig. 5 represents the insulator string overvoltage when the lightning stroke was 31 kA, 5/70 μs. As shown in Fig. 5(a), without EGLA installation, the insulator string overvoltage rises with soil resistivity increasing and flashover happens at the struck tower for the footing resistance more than 500 Ω.m. With soil resistivity increment, lightning current cannot discharge via tower footing resistance, so more back-flashover current flows from insulator string and leads to insulation breakdown. As shown in Fig. 5(b), the EGLA installation improves insulator string overvoltage, and as a consequence, no insulation breakdown takes place. In this situation, discharge current flows through the EGLA instead of the insulator string and prevents insulation failure.

The overvoltage values for static and nonlinear resistances have been shown in Fig. 6. According to the results, overvoltage amplitudes for nonlinear resistance are lower than the static one. Soil ionization varies the flowing current magnitude through the tower footing and so the nonlinear resistance amplitude is lower than the static one. Therefore, during the back flashover event, the EGLA return current for the static resistance is higher than the nonlinear one which causes more overvoltage amplitude.

4.3 Back Flashover Current Investigation

Based on the impact area, the Monte-Carlo simulation has been applied to calculate the lightning flashover rate. Therefore random values of lightning parameters have been generated and considering the EGM model, termination point of the impact area has been

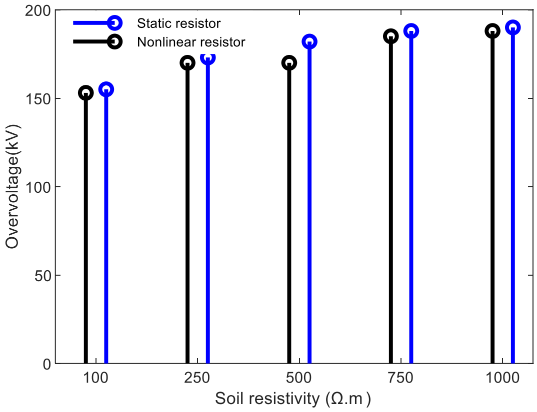

Fig. 6 The insulator string overvoltages with EGLA.

determined for every lightning stroke. According to the impact point, induced overvoltage has been calculated and, SFFOR, BFR, and LFOR are determined after Monte Carlo termination.

$$SFFOR = N_g.100.\ d.\ \frac{F_p}{N},$$
$$BFR = N_g.100.\ d.\ \frac{F_g}{N},$$
$$LFOR = BFR + SFFOR \quad (7)$$

where N is runs number, N_g (flashes/km^2/year) is the ground flash density, F_p and F_g are the number of produced flashovers by lightning surges which strike to phase conductor and shield wire, respectively; and d is the maximum width of determined impact area by EGM.

In this section, the footing resistance effects on the back flashover current from the insulator or EGLA have been investigated. High tower footing resistance causes larger stroke current to be discharged through the installed surge arrester or insulator string. Therefore, a low tower footing resistance is necessary to reduce the insulator overvoltage.

The back flashover currents through the insulator string and EGLA have been shown in Fig. 7. In this case, the lightning surge (31kA 5/70μs) has been hit to shielding wire and the soil resistivity has been chosen 750 Ω.m and 1000 Ω.m. According to Fig. 7(a), due to the high amplitude of soil resistivity, the lightning current did not discharge through the ground resistor and has passed from the insulator string that causing insulation breakdown. However, as shown in Fig. 7(b), after EGLA installing (in parallel with insulator string), the back flashover current flowed through the EGLA instead of the insulator string. Higher stroke magnitude leads to more flowing discharge current from the EGLA and also produce higher energy stress. The passing current through EGLA depends on its absorbed energy. Therefore, the absorbed energy capability of EGLA is one of the main factors which should be considered.

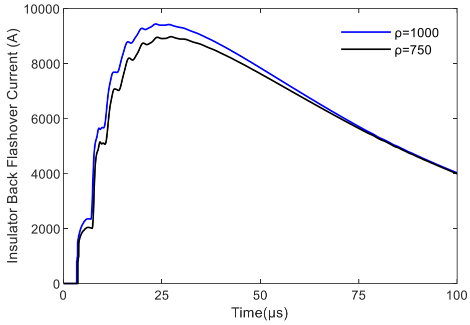

(a)

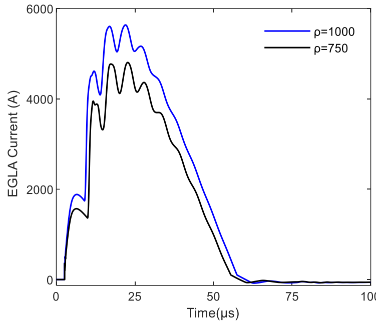

(b)

Fig. 7 Discharge current caused by lightning strokes to shielding wire (31 kA 5/70 μs); a) without EGLA and b) with EGLA.

4.4 EGLA Performance Evaluation

The amount of surge arrester absorbed energy before it fails, is called energy absorption capability. Statistics demonstrate that surge arrester failures created by lightning strikes are about 80% of the total failure number. Therefore, it causes SAs destruction due to the overvoltage effect which has large amplitudes [10]. During overvoltage, the absorbed energy by the arrester relates to different factors such as waveform, amplitude, and overvoltage duration. The following equation has been used to calculate the surge arrester absorbed energy [26]:

$$E = \int_{t_0}^{t} V_s(t).I_s(t).dt \quad (8)$$

where E is the absorbed energy, V_s is the surge arrester voltage, I_s is surge arrester discharge current, and t_0 is the time that lightning appears at surge arrester terminal.

Surge arrester energy absorption capability and its energy stress can be used to investigate the arrester failure risk. It is assumed that the lightning energy distribution is the normal density and so the probability density of energy occurrence can be estimated as follows:

$$f(e) = \frac{1}{\sqrt{2\pi\sigma}} \exp\left[-\frac{(e-e_{50\%})^2}{2\sigma^2}\right] \quad (9)$$

Table 5 The EGLA absorbed energy for lightning stroke (31 kA 5/70 µs) to phase conductor.

Soil resistivity [Ω.m]	EGLA absorbed energy [J]	
	Static resistor	Nonlinear resistor
500	36030	41901
750	28045	37555
1000	26750	33027

Table 6 The EGLA absorbed energy for lightning stroke (31 kA 5/70 µs) to shielding wire.

Soil resistivity [Ωm]	EGLA absorbed energy [J]	
	Static resistor	Nonlinear resistor
500	18720	9530
750	39610	23500
1000	55700	35870

Table 7 The EGLA expected life for lightning strokes to phase conductor (N_i = 5).

EGLA energy [kJ/kV]	Grounding system	Soil resistivity [Ω.m]		
		100	500	1000
6	Nonlinear	6.2	7.5	11.3
	static	7.6	8.6	12.4
8	Nonlinear	8	10.3	13.4
	static	9.8	11.81	14.7
10	Nonlinear	14.2	18.9	22.6
	static	17.4	21.67	24.8

Table 8 The EGLA expected life for lightning strokes to shielding wire (N_i = 5).

EGLA energy [kJ/kV]	Grounding system	Soil resistivity [Ω.m]	
		750	1000
6	Nonlinear	14.7	10.6
	static	10.3	8.1
8	Nonlinear	18.3	15.7
	static	13.8	11.3
10	Nonlinear	26.9	25.5
	static	20.1	22.7

where $f(e)$ is energy happening probability density, $e_{50\%}$ is the probability density of the energy with 50% happening and σ is the standard deviation. The arrester failure probability, $F(e)$, can be approximated by a Weibull cumulative distribution [27]:

$$F_{(e)} = 1 - 0.5(\frac{z}{4}+1)^5, \quad z = (\frac{e}{e_R} - 2.5)/0.375 \tag{10}$$

where e_R is the rated energy capacity and e is the energy withstand capacity. Also (10) is used to calculate surge arrester failure rate and its expected life [28].

$$SA_{FR} = \int F_{(e)}\ f_{(e)}\ d_e \tag{11}$$

$$E_L = \frac{100}{2 \times Ni \times SA_{FR}} \tag{12}$$

where N_i is the number of flashes/100km/year. E_L is the EGLA expected life (year) and SA_{FR} is failure rate (%).

Tower footing resistance variation has been evaluated in this section to analyze its influence on the EGLA discharge energy. The EGLA absorbed energy is represented in Tables 5 and 6 for lightning stroke (31 kA 5/70 µs) to phase conductor and shielding wire. According to Table 5, high resistance leads to a lower stroke current to be discharged through the installed EGLA. Therefore, the calculated absorbed energy decreases as soil resistivity arises in lightning strikes to phase conductor. For the nonlinear resistor, the absorbed energy has a higher amplitude compared to the static resistor. In fact, the nonlinear tower footing resistance has a lower value than the static one, and therefore more current passes the surge arrester and leading to more amount of the absorbed energy.

According to Table 6, more back flashover current passes through EGLA with respect to the soil resistivity and causing more amount of the absorbed energy. Besides, the absorbed energy of the EGLA for the nonlinear resistor is lower than the static one.

Surge arrester selection with an appropriate capability of energy absorption is difficult. Extremely nonlinear voltage stress that has been created by lightning surges and voltage-current characteristics of the SAs are the main restriction factors [27]. Failure probability analysis of a surge arrester is difficult and depends on several parameters including arrester characteristic, surge arrester installation point, impact point of the lightning strokes, and lightning parameters.

Table 7 shows the expected life of EGLA for different energies absorption capabilities. The expected life has been calculated for different soil resistivities. In this situation, lightning surges have been stroked to the phase conductor. Increasing the soil resistivity results in lower energy absorbed by the EGLA and a lower failure rate. As shown in Table 7, the energy absorption capability increment will cause higher estimated life.

The expected life of the EGLA for lightning strokes to shielding wire has been shown in Table 8. The soil resistivity increasing will result in an increment in theEGLA energy. Therefore, the failure rate increases and the expected life decreases. However, as shown in Table 8, increasing energy absorption capability from 6 to 10 kJ/kV leads to the EGLA estimated life increment.

5 Conclusions

EGLA performances have been studied to evaluate the lightning performance of a typical 63 kV transmission line. The soil electrical parameters are also investigated to calculate the back flashover rate. The tower footing resistance is modeled by the constant resistance and the nonlinear resistance whereby the soil ionization varies according to the following current from the tower footing. The obtained results have been represented as follows:

- For the nonlinear and static resistors, the overvoltages values are different. This is due to the soil electrical parameters' dependency on ionization.
- For lightning strikes to the phase conductor, the EGLA absorbed energy has been decreased as soil resistivity increases. Hence, less discharge current flows through the EGLAs and results in more expected life.

For lightning strokes to the shielding wire, the EGLA absorbed energy increases according to the soil resistivity and resulting in more back flashover current. In addition, the expected life has been reduced with soil resistivity increment.

Intellectual Property

The authors confirm that they have given due consideration to the protection of intellectual property associated with this work and that there are no impediments to publication, including the timing of publication, with respect to intellectual property.

Funding

No funding was received for this work.

CRediT Authorship Contribution Statement

M. Khodsuz: Idea & conceptualization, Research & investigation, Data curation, Methodology, Software and simulation, Formal analysis, Verification, Original draft preparation, Revise & editing.

Declaration of Competing Interest

The authors hereby confirm that the submitted manuscript is an original work and has not been published so far, is not under consideration for publication by any other journal and will not be submitted to any other journal until the decision will be made by this journal. All authors have approved the manuscript and agree with its submission to “Iranian Journal of Electrical and Electronic Engineering”.

References

[1] A. Borghetti, F. Napolitano, C. A. Nucci, and F. Tossani, “Influence of the return stroke current waveform on the lightning performance of distribution lines,” *IEEE Transactions on Power Delivery*, Vol. 32, No. 4, pp. 1800–1808, 2017.

[2] I. A. Metwally, M. Eladawy, and E. A. Feilat, “Online condition monitoring of surge arresters based on third-harmonic analysis of leakage current,” *IEEE Transactions on Dielectrics and Electrical Insulation*, Vol. 24, No. 4, pp. 2274–2281, 2017.

[3] Z. N. Stojanovic and Z. M. Stojkovic, “Evaluation of MOSA condition using leakage current method,” *International Journal of Electrical Power and Energy Systems*, Vol. 52, No. 1, pp. 87–95, 2013.

[4] M. Khodsuz, M. Mirzaie, and S. M. Seyyedbarzegar, “Metal oxide surge arrester condition monitoring based on analysis of leakage current components,” *International Journal of Electrical Power and Energy Systems*, Vol. 66, No. 1, pp. 188–193, 2015.

[5] J. A. Martinez, F. Gonzalez, P. Chowdhuri, “Calculation of lightning flashover rates of overhead distribution lines: A comparative study,” in *Proceedings of Power Engineering Society Summer Meeting*, 2000.

[6] P. Liu, G. N. Wu, B. Sui, R. F. Li, and X. B. Cao, “Modeling lightning performance of transmission systems using PSCAD,” in *International Conference on High Voltage Engineering and Application, Chongqing*, pp. 168–171, 2008.

[7] J. A. Martinez and F. C. Aranda, “Lightning performance analysis of overhead transmission lines using the EMTP,” *IEEE Transaction on Power Delivery*, Vol. 20, No. 3, pp. 2200–2210, 2005.

[8] S. A. Hosseini, M. Mirzaie, and T. Barforoshi, “Impact of surge arrester number and placement on reliability and lightning overvoltage level in high voltage substations,” *International Journal of Electrical Power and Energy Systems*, Vol. 65, No. 1, pp. 146–158, 2015.

[9] J. He, S. Chen, R. Zeng, J. Hu, and C. Deng, “Development of polymeric surge ZnO arresters for 500-kV compact transmission line,” *IEEE Transaction on Power Delivery*, Vol. 21, No. 1, pp. 113–120, 2006.

[10] M. E. Ahmadi, M. Niasati, and M. R. Barzegar-Bafrooei, “Enhancing the lightning performance of overhead transmission lines with optimal EGLA and downstream shield wire placement in mountainous areas: a complete study,” *IET Science, Measurement and Technology*, Vol. 14, No. 5, pp. 564–575, 2020.

[11] T. H. Pham, S. A. Boggs, H. Suzuki, and T. Imai, "Effect of externally gapped line arrester placement on insulation coordination of a twin-circuit 220 kV line," *IEEE Transactions on Power Delivery*, Vol. 27, No. 4, pp. 1991–1997, 2012.

[12] F. Giraudet, "Various benefits for line surge arrester application and advantages of externally gapped line arresters," *Power Research*, Vol. 15, No. 2, pp. 136–144, 2019.

[13] S. Chen, J. Guo, C. Hu, K. Li, J. Jia, and Y. Xu, "Study on the influence of arrester unit parameters and gap structure on impulse discharge voltage of EGLA," in *12th International Conference on the Properties and Applications of Dielectric Materials (ICPADM)*, pp. 566–569, 2018.

[14] C. A. Christodoulou, L. Ekonomou, N. Papanikolaou, and I. F. Gonos, "Effect of the grounding resistance to the behaviour of high-voltage transmission lines surge arresters," *IET Science, Measurement and Technology*, Vol. 8, No. 6, pp. 470–478, 2014.

[15] A. H. A. Bakar, D. N. A. Talib, H. Mokhlis, and H. A. Illias, "Lightning back flashover double circuit tripping pattern of 132 kV lines in Malaysia," *International Journal of Electrical Power and Energy Systems*, Vol. 45, No. 1, pp. 235–241, 2013.

[16] D. Stanchev, "Model study of lightning overvoltages in substation due to back flashover of overhead transmission line 220 kV," in *10th Electrical Engineering Faculty Conference (BulEF)*, Sozopol, Bulgaria, 2018.

[17] D. Wang, B. He, W. Zhong, B. Lin, D. Wang, and T. Li, "Application and analysis for surge arrester on lightning protection of distribution network," in *MATEC Web of Conferences*, Vol. 34, p. 06002, 2016.

[18] N. H. Nor Hassan, A. H. Abu Bakar, H. Azil Illias, S. Abd Halim, H. Mokhlis, and V. Terzija, "Analysis of discharge energy on surge arrester configurations in 132 kV double circuit transmission lines," Vol. 139, No. 1, pp. 103–111, 2019.

[19] R. Shariatinasab, J. Gholinezhad, and K. Sheshyekani, "Estimation of energy stress of surge arresters considering the high-frequency behavior of grounding systems," *IEEE Transactions on Electromagnetic Compatibility*, Vol. 60, No. 4, pp. 917–925, 2018.

[20] P. Chowdhuri, J. G. Anderson, W. A. Chisholm, T. E. Field, M. Ishii, J. A. Martinez, M. B. Marz, J. McDaniel, T. E. McDermott, A. M. Mousa, and T. Narita, "Parameters of lightning strokes: A review," *IEEE Transaction on Power Delivery*, Vol. 20, No. 1, pp. 346–358, 2005.

[21] F. Heidler, J. M. Cvetic, and B. V. Stanic, "Calculation of lightning current parameters," *IEEE Transaction on Power Delivery*, Vol. 14, No. 2, pp. 399–404, 1999.

[22] A. M. Mousa and K. D. Srivastava, "The implications of the electro geometric model regarding effect of height of structure on the median amplitude of collected lightning strokes," *IEEE Transaction on Power Delivery*, Vol. 4, pp.1450–1460, 1989.

[23] A. Ametani and T. Kawamura, "A method of a lightning surge analysis recommended in Japan using EMTP," *IEEE Transaction on Power Delivery*, Vol. 20, No. 2, pp. 867–875, 2005.

[24] Z. G. Datsios, P. N. Mikropoulos, and T. E. Tsovilis, "Estimation of the minimum shielding failure flashover current for first and subsequent lightning strokes to overhead transmission lines," *Electric Power System Research*, Vol. 113, No. 1, pp. 141–150, 2014.

[25] J. A. Martinez and D. W. Durbak, "Parameter determination for modeling systems transients—Part V: Surge arresters," *IEEE Transaction on Power Delivery*, Vol. 20, No. 3, pp. 2073–2078, 2005.

[26] K. E. Merrill and G. T. Heydt, "The calculation of energy dissipation in metal oxide varistors for power distribution applications," *IEEE Transactions on Power Systems*, Vol. 34, No. 5, pp. 3967–3969, 2019.

[27] N. A. Sabiha, F. Mahmood, and A. M. Abd-Elhady, "Failure risk assessment of surge arrester using paralleled spark gap," *IEEE Access*, Vol. 8, No. 1, pp. 346–358, 2020.

[28] L. Montanes, M. G. Garsia, M. Sanz, and M. A. Garsia, "An improvement for the selection of surge arresters based on the evaluation of the failure probability," *IEEE Transaction on Power Delivery*, Vol. 17, No. 1, pp. 123–128, 2002.

M. Khodsuz was born in Sari, Iran in 1985. She received the B.Sc. and M.Sc. degree in Power Engineering both from Mazandaran University of Technology in 2007 and 2010, respectively and Ph.D. degree in Power Engineering from Babol University of Technology in High Voltage Engineering in 2015. She works as an Assistant Professor at University of Science and Technology of Mazandaran. Her research interests are electric and magnetic field analysis, high-voltage engineering, reliability, high voltage equipment condition diagnostic, and power quality.